WILEY-VCH

DOI: 10.1002/ (please add manuscript number)
Article type: Communication

Title: **Fast High-Responsivity Few-Layer $MoTe_2$ Photodetectors**

*Tobias J. Octon, V. Karthik Nagareddy, S. Russo, Monica F. Craciun, C. David Wright**

T. J. Octon, V. K. Nagareddy, Prof. S Russo, Prof. M. F. Craciun, Prof. C. D. Wright
College of Engineering, Mathematics and Physical Sciences
Centre of Graphene Science
University of Exeter
Exeter, EX 4 4QF, United Kingdom
E-mail: david.wright@exeter.ac.uk

Keywords: molybdenum ditelluride, field effect transistor, photodetection, 2D materials, fast photo-response

The Transition Metal Dichalcogenide $MoTe_2$ is fabricated via mechanical exfoliation into few-layer Field Effect Transistors (FETs) having a hole mobility of 2.04 $V/cm^2/s$. Four-layer $MoTe_2$ FETs show a high photoresponsivity of 6 A/W and a response time, at around 160 µs, over 100 times faster than previously reported for $MoTe_2$. Few-layer $MoTe_2$ thus appears as a strong candidate for high speed and high sensitivity photodetection applications.

In the search for optoelectronic materials suited to flexible[1] and transparent[2] electronics and photonics applications, transition metal dichalcogenide (TMDC) materials are particularly attractive since they can be fabricated in two-dimensional form with a direct band-gap electronic structure making them potentially suitable for high-photoresponsivity applications.[3–5] However, for virtually all of the TMDCs reported to date a very slow photoresponse has been observed, often of the order of seconds (or tens of milliseconds at best), limiting their application potential to conditions of static or very slowly varying optical excitation.[6,7] Here

we report on the optoelectronic properties of few-layer $MoTe_2$ devices in which we observe the simultaneous combination of a high photoresponsivity and a fast photoresponse.

$MoTe_2$ has shown similar electrical properties to other TMDCs including the highly utilized MoS_2.[8–13] In few-layer $MoTe_2$ the band gap is in the range 1 - 1.1 eV, extending to near infrared the range of band gaps available for TMDCs.[14] The photoconductivity of MoS_2 has been well researched,[6,7,15–20] however $MoTe_2$ has only just begun to be explored for its optoelectronic properties and $MoTe_2$ flakes of thicknesses in the one to four layer range have not previously been studied optoelectronically.[9,21–23] In this paper we fabricate four-layer $MoTe_2$ into Field Effect Transistors (FETs) and find this thickness of $MoTe_2$ to be a fast, sensitive photodetector with a photoresponsivity of ~6 A/W and a photoresponse time of around 160 μs, approximately 125 times faster than previous reported measurements on $MoTe_2$ devices.[22,23]

$MoTe_2$ flakes were deposited onto Si/SiO_2 (with SiO_2 thickness of 300 nm) for fabrication into FETs. Flakes were deposited by mechanical exfoliation[24] and identified using optical microscopy, Raman spectroscopy and atomic force microscopy (AFM) a method which has proven well suited for characterizing this material.[11,14,25] We used 4-layer flakes for our photocurrent measurements as Pradhan et al. showed that the use of few-layer TMDCs can reduce photocurrent response times while keeping photoresponsivity high.[26] Work done by Lezama et al. also shows the transition of $MoTe_2$ to a direct band gap beginning at a flake thickness of 4-layers.[5] In **Figure 1**a, an optical microscopy image of a $MoTe_2$ flake of thickness from 1-5 layers is shown; the difference in flake thickness is observed clearly in the optical contrast. In Figure 1b an AFM image of the same flake in Figure 1a is shown, with the height profile along the dashed line being shown in Figure 1c. In Figure 1d Raman spectroscopy of flakes from 1 to 4 layers thick are shown using a 532 nm laser at 30 μW and a grating of 2400 grooves mm^{-1}. The Raman peak positions are in agreement with Yamamoto et al. for the

E^1_{2g}, A_{1g} and B^1_{2g} peaks, meaning we are confident in using Raman spectroscopy to identify flake thickness of $MoTe_2$.[5,14,25] In Figure 1e the ratio of areas of the E^1_{2g} and B^1_{2g} Raman peaks as a function of flake thickness is displayed; this ratio is subsequently used to confirm the flake thickness of $MoTe_2$ using only Raman spectroscopy.

After thorough characterization of $MoTe_2$ flake thickness, two terminal FET devices, as shown schematically in **Figure 2a**, were fabricated as described in the Experimental Section. Figure 2b and 2c show optical microscopy images of a typical flake before and after deposition of the electrodes. In Figure 2d the output characteristics of a 4-layer $MoTe_2$ FET are shown: increased conduction is shown as gate voltage decreases from +10 to -30 V, showing the device is hole doped since it is entering the ON state with a negative gate voltage applied. In Figure 2e the transfer characteristics of the same four-layer device are displayed; hysteresis is observed as the gate voltage is swept from +50 V to -50 V and back, indicating the existence of trap states between the $MoTe_2/SiO_2$ interface.[6] Our transfer characteristic displayed hole conduction which has been observed for $MoTe_2$ few-layer FETs[8,9], although ambipolar transport has also been observed in the literature for $MoTe_2$ devices.[10,11,21,27] In Fig. 2(c) the field effect mobility, μ_{FE}, (calculated using the equation $\mu_{FE} = (\frac{L}{W})(\frac{d}{\varepsilon_0 \varepsilon_r V_{ds}})(\frac{\Delta I_{ds}}{\Delta V_g})$, where L and W are the length and width of the channel respectively, d is the oxide thickness, ε_0 and ε_r are the permittivity of free space and the relative permittivity of SiO_2, V_{ds} is the drain to source voltage and the last term is the inverse slope of the transfer characteristic in the linear regime of the ON state) is 2.04 and 0.86 $cm^2/V/s$ for the up sweep and down sweep respectively. This hole mobility is comparable to that reported for other few-layer $MoTe_2$ FETs in the literature, e.g. 0.3 $cm^2/V/s$ in ref. [10] and a maximum of 1.5 $cm^2/V/s$ in [21]. It is however somewhat lower than in some studies, e.g. 10 $cm^2/V/s$ in ref. [11] and 26 $cm^2/V/s$ in ref. [27], most likely due to a relatively high contact resistance in our case (~2.5 $M\Omega \cdot \mu m$, as estimated from the slope of our I_{DS}-V_{DS}

curve at V_g = -30 V) along with the fact that these latter studies used ionic gates. For our 4-layer devices we saw only hole conduction, as observed by others for few-layer $MoTe_2$ FETs [8,9]. We note however that electron transport has also been reported in many $MoTe_2$ studies.[10,11,21,27]; while we did not observe any electron transport in our 4-layer devices, we did see an electron contribution in thicker devices (8-layers) (See **Figure S1**).

In **Figure 3** the output and transfer characteristics were measured under illumination by a 685 nm (1.8 eV) laser in a custom-built photocurrent measurement setup (schematic shown in **Figure S2**) with the laser focused through a 50x objective lens, capable of creating spot sizes of 1.5 μm (note that this 4-layer device was different to that used for the results of Figure 2, but both devices showed very similar electrical characteristics). For all photocurrent measurements the laser spot size was focused at the center of the $MoTe_2$ channel and illuminated both metal electrodes (though we note, as observed in ref. [18], that the photocurrent was locally enhanced at the electrode-channel interfaces, see **Figure S3**).

Figure 3a shows the output characteristic for various illumination powers and for zero back gate voltage. An increase in I_{ds} of 15 nA, compared to the dark measurement, is observed using 25 μW illumination at V_{ds} = 1 V, equating to a photoresponsivity of 0.42 mA/W. Figure 3b shows the dependence of the photocurrent on illumination power at V_{ds}= 5 and V_g = 0 V. Our linear fit provides a power dependence of 0.92 ± 0.04. In Figure 3c the transfer characteristic under 400 nW, 685 nm laser illumination and in the dark is shown. From this figure, we measure a two orders of magnitude drop in the photoconductivity during the gate sweep. At -40 V_g (ON state), the device exhibits high photocurrent due to a change in threshold voltage (V_T) of the device with illumination. This mechanism, associated with the photovoltaic effect, is called photogating and has been observed in many semiconductor photodetectors.[19,28,29] The explanation for photogating in a hole doped device is that photogenerated electrons are captured in trap states causing the potential barrier at the interface

between $MoTe_2$ and the Cr/Au electrode to decrease. The electric field is reduced from the accumulated charge, allowing holes to travel through the circuit more freely increasing conduction.[28] At +40 V_g (OFF state) there is no increased photocurrent from photogating so the photoresponsivity in the OFF state is magnitudes lower than in the ON state. In Fig. 3(d) the maximum recorded photoresponsivity of the 4-layer flake is shown to be 6 A/W (at -40 V_g) and depends heavily upon gate voltage. Recent studies on $MoTe_2$ heterostructures have recorded much lower photoresponsivities in the range of 20 - 600 mA/W, [22,23] although one very recent study (carried out in parallel with the work reported in this paper) on the photocurrent in $MoTe_2$ using Au contacts has found a high photoresponsivity of 2560 A/W.[21] Such variations in reported photoreponsivities reflect a wide variation in the measurement conditions used. Photoresponsivity depends of course on (i) the number of excitons generated (which is dependent on the density of charge carriers and the excitation energy) and (ii) the mobility of the charge carriers (which determines how fast they are able to be collected at the contacts). In ref. [9], for example, a low photoresponsivity was recorded since measurements were carried out in the subthreshold region where the carrier (hole in this case) mobility is low. In ref. [21], by contrast, measurements were carried out well above threshold (high gate voltages of 80 V) enhancing an already high carrier (electrons in this case) mobility, and high excitation energies (2.6 eV) were also used. Since we used moderate gate voltages (40 V) and moderate excitation energies (1.8 eV), it is perhaps no surprise that our recorded photoresponsivity falls between those of these earlier works. Indeed, we would expect further increases in the photoresponsivity of our devices should we use higher gate voltages[21,30] and higher excitation energies (both of which would increase the number of excitons generated). We might also improve the photoresponsivity by reducing the contact resistance (by using different contact materials) so as to increase the carrier mobility. The use of an alternative

dielectric, e.g. h-BN, might also improve carrier mobility (and so photoresponsivity), as shown by Withers et al. for WS_2 few-layer FET devices.[31]

Finally, we measured the speed of the photoresponse of the four-layer $MoTe_2$ device by modulating the laser with a square wave at 178 Hz and recording the photocurrent (at V_{ds} = 5 V and V_g = 0 V). The modulated laser waveform and the resulting photocurrent are shown in **Figure 4**a. In Figure 4b and 4c we show zoomed-in regions corresponding to the turn-on and turn-off of the laser, from which we can determine the rise and fall times for the photocurrent. The rise time (defined here as the time taken to go from 10% to 90% of the total photocurrent) is 160 μs and the fall time (defined similarly as the time taken to from 90% to 10% of the total photocurrent) is 300 μs. Such a photoresponse is considerably faster than previously reported for $MoTe_2$, with values of 25 ms being typically observed by others.[22,23]

Indeed, in Figure 4d we summarize the photoresponsivity and the photoresponse time for a wide range of TMDCs reported in the literature (full details of wavelengths used, operating conditions and layer thicknesses of references is given in **Table S1**), where it can be seen that our $MoTe_2$ devices are amongst the fastest of all, while still competitive in terms of photoresponsivity.

We believe that the fast photoresponse we observe is potentially due to three reasons: the thickness of our photodetectors, the crystal quality and the sampling rate/laser rise time used in our photoresponse measurements. We used four-layer flakes in our study, and other similar thickness TMDCs devices have previously shown a fast photoresponse[26,32] whereas using monolayer flakes appears to hamper the photoresponse speed (see Table S1 for full details of flake thickness in correlation to response speeds). We also note that for the fastest (to our knowledge) reported TMDC photoresponse time reported to date, for SnS_2 devices[33], the crystal quality was shown to play a key role in determining the speed of response. Finally, and perhaps surprisingly, it appears that in many cases the response time reported in the literature

is adversely affected by the experimental arrangement used to measure it – often the laser is modulated by a mechanical chopper wheel that limits the rise time of the laser excitation itself, so limiting the measured photoresponse time (in contrast, our laser is directly electrically modulated, and an ultra-fast digital oscilloscope is used to capture the photodetector output).

To summarize, we have fabricated four layer $MoTe_2$ FETs and performed optoelectronic tests including output and transfer characteristics with and without 685 nm laser illumination. We find that $MoTe_2$ is suitable for high photoresponsivity (6 A/W) and fast photoresponse applications (160 μs switching speed) and performs well compared to other TMDCs. We see that $MoTe_2$ exhibits the same mechanisms as traditional semiconductor photodetectors with changes in threshold voltage observed in the ON state and photoconductive effects in the OFF state. The (optical) power dependence of the photocurrent suggests photocarrier generation in few-layer MoTe2 devices is photovoltaically dominated at zero gate bias, making them potentially suitable for solar cell type applications.

Experimental Section

Device Fabrication: $MoTe_2$ flakes were used to fabricate a FET device on 285 nm-thick SiO_2/Si subtrates. Substrates were cleaned by heating in acetone, followed by sonication in acetone and isopropanol and dried by N_2. Bulk α-$MoTe_2$ (from HQ graphene) was exfoliated onto the cleaned substrates and flakes were searched for manually using an optical microscope. The electrodes were patterned by electron beam lithography and 5 nm thick Ti followed by 50 nm thick Au were deposited using a sputtering system. For the lift-off process a solution of isoproponol, methylisobutylketone and methylethylketone in a 15:5:1 ratio was used. Devices were annealed in an Ar/H_2 (90/10%) environment at 200 ^{0}C for 2 hours to remove PMMA residues from lithography and improve device performance. All fabrication steps took place in ambient conditions but care was taken to minimize the total exposure to less than 3 hours due

to the issues of oxidation experimentally observed for monolayer $MoTe_2$.[34] Devices were stored in a vacuum dessicator and no change in the optical contrast or Raman spectra of devices was observed after fabrication.

Electrical and Optoelectrical measurements: Output and transfer characteristics of the 4-layer $MoTe_2$ flake devices were measured in DC using a custom built electrical test station (see Figure S1). A DC voltage source (Xitron 2000) supplied the source-drain bias across the device, another DC voltage source was used to apply the gate voltage (Keithley 2700) and the current across the channel was measured using a multimeter (Agilent 34401A). An intergrated laser and optical microscope with a 50x lens was used for photocurrent measurements with a 685 nm laser. Modulation of the laser was performed using a function generator which created square wave pulses. An oscilloscope was used to record the output of the device and modulation of the laser to obtain the time resolved photo response of the devices.

Acknowledgements

CDW would like to acknowledge funding via EPSRC grants EP/M015173/1 and EP/M015130/1. TJO acknowledges funding from the EPSRC Centre for Doctoral Training in Metamaterials, grant number EP/L015331/1.

Received: ((will be filled in by the editorial staff))
Revised: ((will be filled in by the editorial staff))
Published online: ((will be filled in by the editorial staff))

[1] A. Castellanos-Gomez, M. Poot, G. A. Steele, H. S. J. Van Der Zant, N. Agraït, G. Rubio-Bollinger, *Adv. Mater.* **2012**, *24*, 772.

[2] P. Tonndorf, R. Schmidt, P. Böttger, X. Zhang, J. Börner, A. Liebig, M. Albrecht, C. Kloc, O. Gordan, D. R. T. Zahn, S. M. de Vasconcellos, R. Bratschitsch, *Opt. Express* **2013**, *21*, 4908.

[3] K. F. Mak, C. Lee, J. Hone, J. Shan, T. F. Heinz, *Phys. Rev. Lett.* **2010**, *105*, 136805.

[4] A. Splendiani, L. Sun, Y. Zhang, T. Li, J. Kim, C.-Y. Chim, G. Galli, F. Wang, *Nano Lett.* **2010**, *10*, 1271.

[5] I. Lezama, A. Arora, A. Ubaldini, E. Giannini, A. F. Morpurgo, *Nano Lett.* **2015**, *15*, 2336.

[6] O. Lopez-Sanchez, D. Lembke, M. Kayci, A. Radenovic, A. Kis, *Nat. Nanotechnol.* **2013**, *8*, 497.

[7] Z. Yin, H. Li, H. Li, L. Jiang, Y. Shi, Y. Sun, G. Lu, Q. Zhang, X. Chen, H. Zhang, *ACS Nano* **2011**, *6*, 74.

[8] N. R. Pradhan, D. Rhodes, S. Feng, Y. Xin, S. Memaran, B. Moon, *Am. Chem. Soc.* **2014**, *8*, 5911.

[9] S. Fathipour, N. Ma, W. S. Hwang, V. Protasenko, S. Vishwanath, H. G. Xing, H. Xu, D. Jena, J. Appenzeller, A. Seabaugh, *Appl. Phys. Lett.* **2014**, *105*, 192101.

[10] Y.-F. Lin, Y. Xu, S.-T. Wang, S.-L. Li, M. Yamamoto, A. Aparecido-Ferreira, W. Li, H. Sun, S. Nakaharai, W.-B. Jian, K. Ueno, K. Tsukagoshi, *Adv. Mater.* **2014**, *26*, 3263.

[11] I. G. Lezama, A. Ubaldini, M. Longobardi, E. Giannini, C. Renner, A. B. Kuzmenko, A. F. Morpurgo, *2D Mater.* **2014**, *1*, 021002.

[12] B. Radisavljevic, A. Radenovic, J. Brivio, V. Giacometti, A. Kis, *Nat. Nanotechnol.* **2011**, *6*, 147.

[13] J. Kumar, M. A. Kuroda, M. Z. Bellus, S.-J. Han, H.-Y. Chiu, *Appl. Phys. Lett.* **2015**, *106*, 123508.

[14] C. Ruppert, O. B. Aslan, T. F. Heinz, *Nano Lett.* **2014**, *14*, 6231.

[15] M. Buscema, M. Barkelid, V. Zwiller, H. S. J. Van Der Zant, G. A. Steele, A. Castellanos-gomez, *Nano Lett.* **2013**, *13*, 358.

[16] M. Fontana, T. Deppe, A. K. Boyd, M. Rinzan, A. Y. Liu, M. Paranjape, P. Barbara, *Sci. Rep.* **2013**, *3*, 1634.

[17] W. Zhang, J.-K. Huang, C.-H. Chen, Y.-H. Chang, Y.-J. Cheng, L.-J. Li, *Adv. Mater.* **2013**, *25*, 3456.

[18] C. Wu, D. Jariwala, V. K. Sangwan, T. J. Marks, M. C. Hersam, L. J. Lauhon, *J. Phys. Chem. Lett.* **2013**, *4*, 2508.

[19] M. M. Furchi, D. K. Polyushkin, A. Pospischil, T. Mueller, *nano Lett.* **2014**, *14*, 6165.

[20] Y. Zhang, H. Li, L. Wang, H. Wang, X. Xie, S.-L. Zhang, R. Liu, Z.-J. Qiu, *Sci. Rep.* **2015**, *5*, 7938.

[21] L. Yin, X. Zhan, K. Xu, F. Wang, Z. Wang, Y. Huang, Q. Wang, C. Jiang, J. He, *Appl. Phys. Lett.* **2016**, *108*, 043503.

[22] M. Kuiri, B. Chakraborty, A. Paul, S. Das, A. K. Sood, A. Das, *Appl. Phys. Lett.* **2016**, *108*, 063506.

[23] A. Pezeshki, S. H. H. Shokouh, T. Nazari, K. Oh, S. Im, *Adv. Mater.* **2016**, DOI 10.1002/adma.201504090.

[24] K. S. Novoselov, A. K. Geim, S. V Morozov, D. Jiang, Y. Zhang, S. V Dubonos, I. V Grigorieva, A. A. Firsov, *Science (80-.).* **2004**, *306*, 666.

[25] M. Yamamoto, S. T. Wang, M. Ni, Y. F. Lin, S. L. Li, S. Aikawa, W. Bin Jian, K. Ueno, K. Wakabayashi, K. Tsukagoshi, *ACS Nano* **2014**, *8*, 3895.

[26] N. Pradhan, J. Ludwig, Z. Lu, D. Rhodes, M. M. Bishop, K. Thirunavukkuarasu, S.

McGill, D. Smirnov, L. Balicas, *ACS Appl. Mater. Interfaces* **2015**, *7*, 12080.

[27] H. Xu, S. Fathipour, E. W. Kinder, A. C. Seabaugh, S. K. Fullerton-Shirey, *ACS Nano* **2015**, 5, 4900.

[28] A. Madjar, P. R. Herczfeld, A. Paolella, *IEEE Trans. Microw. Theory Tech.* **1992**, *40*, 1681.

[29] Y. Takanashi, K. Takahata, Y. Muramoto, *IEEE Trans. Electron Devices* **1999**, *46*, 2271.

[30] A. K. M. Newaz, D. Prasai, J. I. Ziegler, D. Caudel, S. Robinson, R. F. Haglund, K. I. Bolotin, *Solid State Commun.* **2013**, *155*, 49.

[31] F. Withers, T. H. Bointon, M. F. Craciun, S. Russo, *ACS Nano* **2013**, *7*, 5052.

[32] D. S. Tsai, K. K. Liu, D. H. Lien, M. L. Tsai, C. F. Kang, C. A. Lin, L. J. Li, J. H. He, *ACS Nano* **2013**, *7*, 3905.

[33] G. Su, V. G. Hadjiev, P. E. Loya, J. Zhang, S. Lei, S. Maharjan, P. Dong, P. M. Ajayan, J. Lou, H. Peng, *Nano Lett.* **2015**, *15*, 506.

[34] B. Chen, H. Sahin, A. Suslu, L. Ding, M. Bertoni, F. M. Peeters, *ACS Nano* **2015**, *9*, 5326.

[35] W. Choi, M. Y. Cho, A. Konar, J. H. Lee, G.-B. Cha, S. C. Hong, S. Kim, J. Kim, D. Jena, J. Joo, S. Kim, *Adv. Mater.* **2012**, *24*, 5832.

[36] N. Perea-López, Z. Lin, N. R. Pradhan, A. Iñiguez-Rábago, A. Laura Elías, A. McCreary, J. Lou, P. M. Ajayan, H. Terrones, L. Balicas, M. Terrones, *2D Mater.* **2014**, *1*, 011004.

[37] A. Abderrahmane, P. J. Ko, T. V Thu, S. Ishizawa, T. Takamura, A. Sandhu, *Nanotechnology* **2014**, *25*, 365202.

[38] Y. Chang, O. W. Zhang, O. Y. Zhu, Y. Han, J. Pu, J. Chang, W. Hsu, *ACS Nano* **2014**, *8*, 8582.

[39] J. Xia, X. Huang, L.-Z. Liu, M. Wang, L. Wang, B. Huang, D.-D. Zhu, J.-J. Li, C.-Z. Gu, X.-M. Meng, *Nanoscale* **2014**, *6*, 8949.

[40] E. Zhang, Y. Jin, X. Yuan, W. Wang, C. Zhang, L. Tang, S. Liu, P. Zhou, W. Hu, F. Xiu, *Adv. Funct. Mater.* **2015**, *25*, 4076.

[41] N. Perea-Lopez, A. L. Elias, A. Berkdemir, A. Castro-Beltran, H. R. Gutierrez, S. Feng, R. Lv, T. Hayashi, F. Lopez-Urias, S. Ghosh, B. Muchharla, S. Talapatra, H. Terrones, M. Terrones, *Adv. Funct. Mater.* **2013**, *23*, 5511.

[42] N. Huo, S. Yang, Z. Wei, S.-S. Li, J.-B. Xia, J. Li, *Sci. Rep.* **2014**, *4*, 5209.

[43] W. Zhang, M. Chiu, C.-H. Chen, W. Chen, L. Li, A. T. S. Wee, *ACS Nano* **2014**, *8*, 8653.

[44] D. J. Groenendijk, M. Buscema, G. A. Steele, R. Bratschitsch, H. S. J. Van Der Zant, A. Castellanos-gomez, **2014**, *14*, 5846.

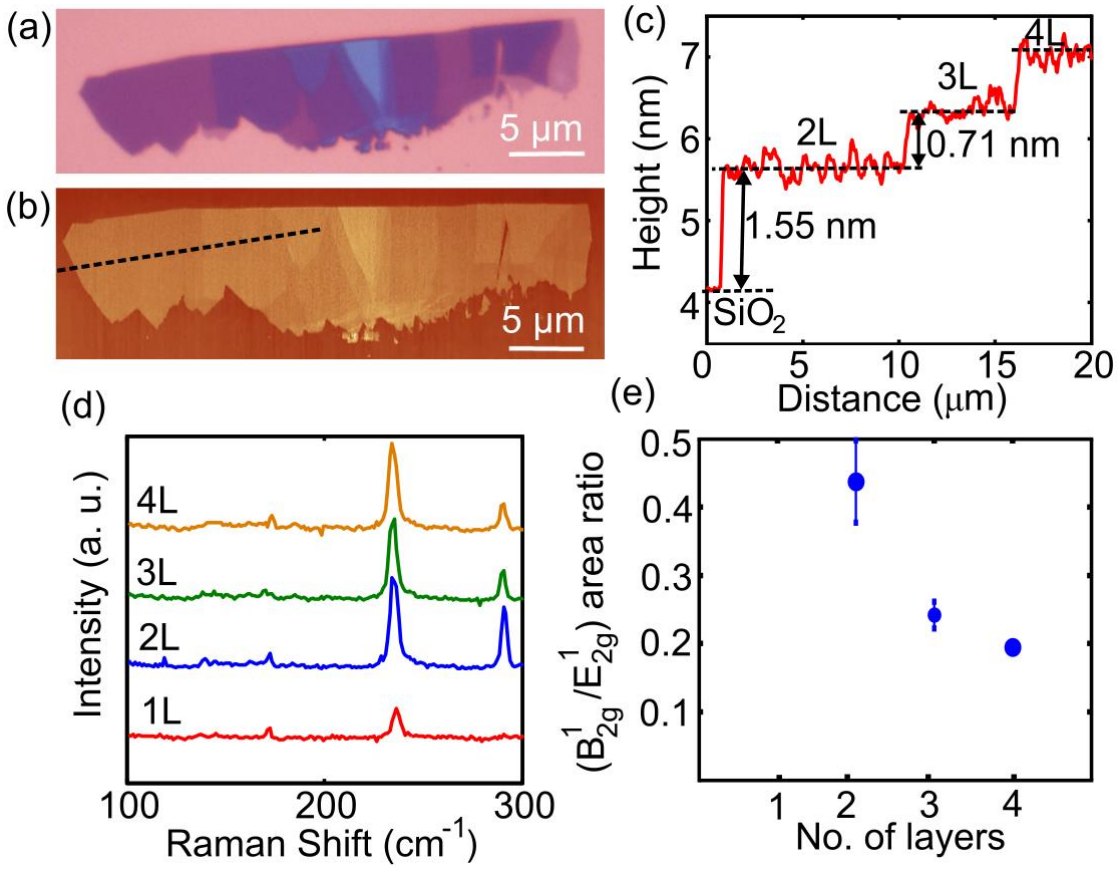

Figure 1. (a) Optical microscopy image of 4 layer flake used in our photocurrent study at 100x magnification after and before fabrication. (b) AFM image showing difference in heights between layers of ~0.7 nm. (c) AFM profile along the dashed black line in Fig. 1(b). (d) Raman spectroscopy of 1 – 4 layer thick $MoTe_2$ flakes with a 532 nm laser. (e) Peak area ratios of E^1_{2g} and B^1_{2g} against layer thickness.

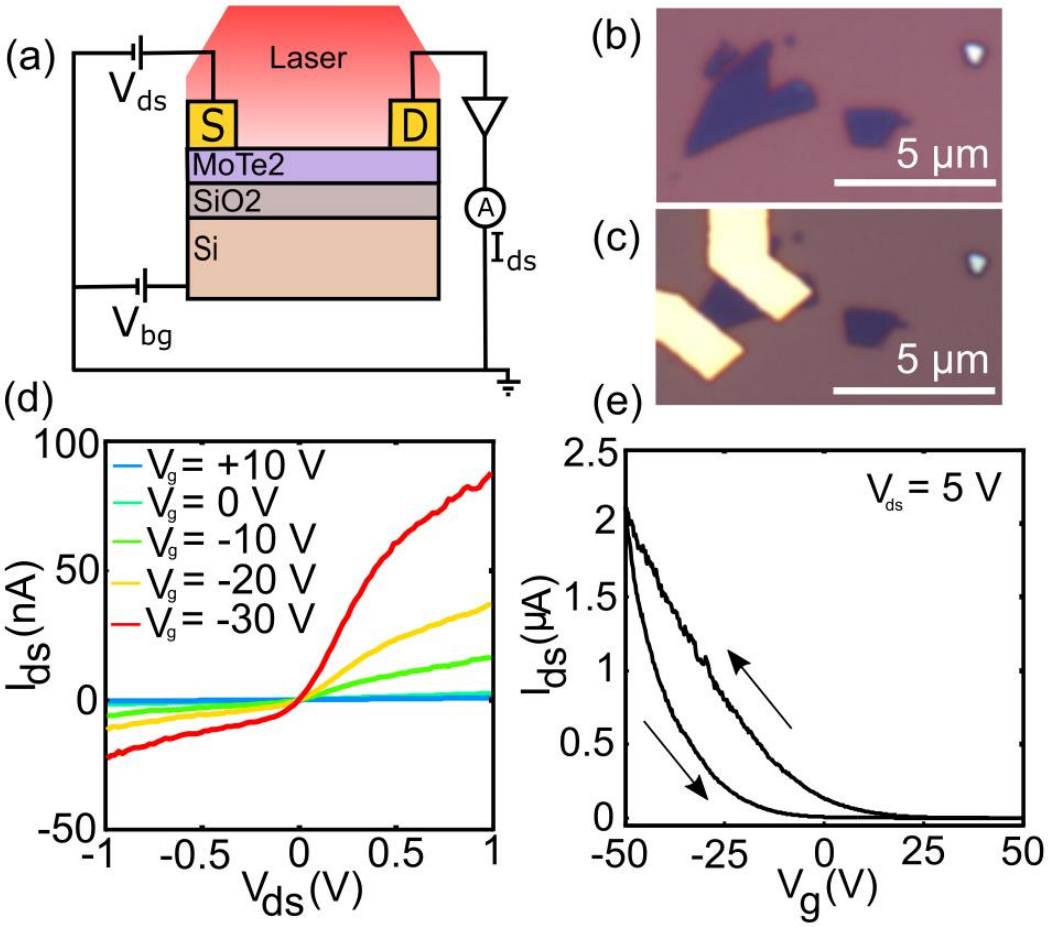

Figure 2. (a) Schematic of $MoTe_2$ few layer FET. (b) & (c) Four layer flake before and after device fabrication. (d) V_{ds} vs. I_{ds} at V_g values from +10 to -30 V. (e) V_g vs. I_{ds} at V_{ds} = 5 V.

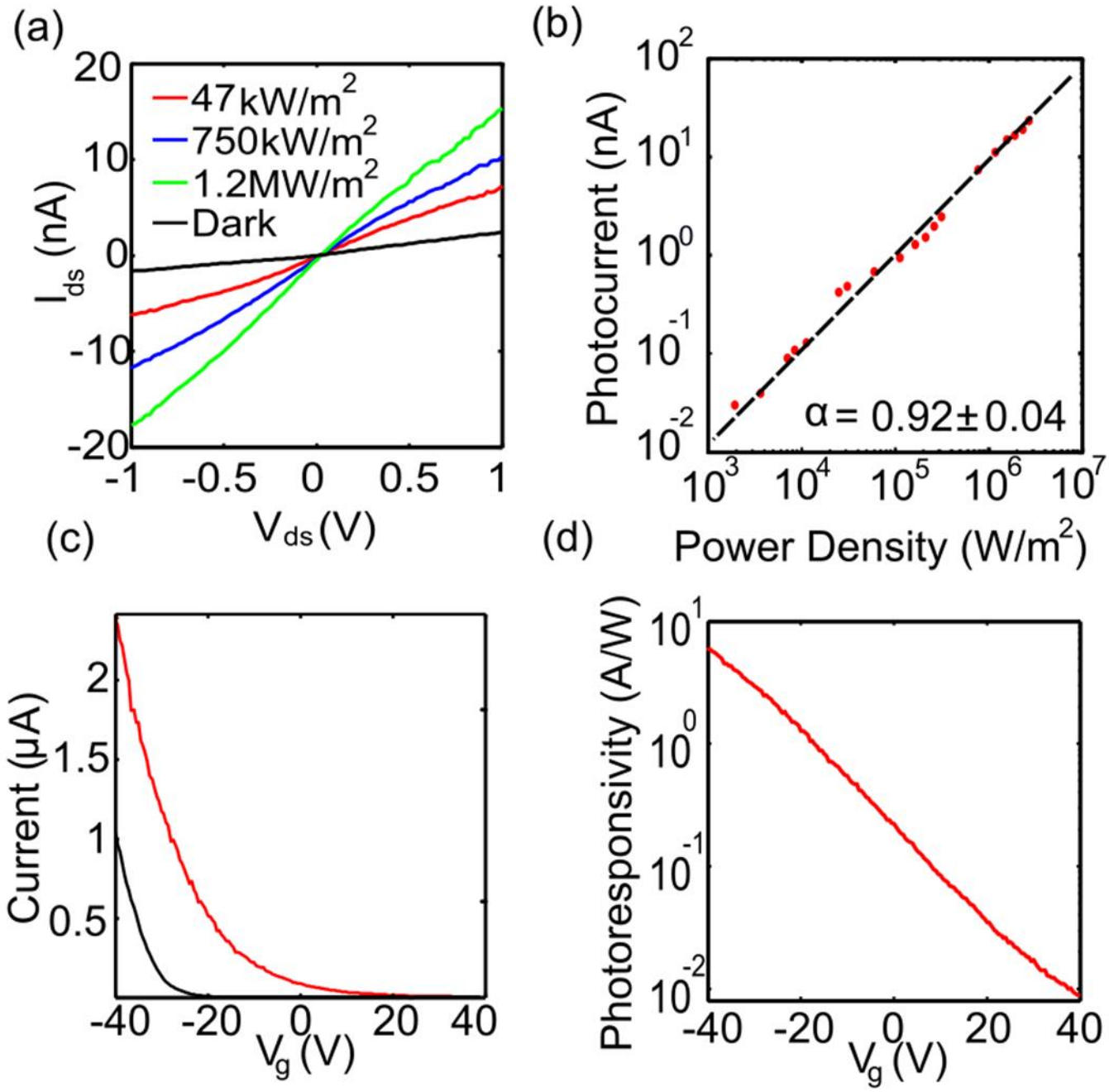

Figure 3. (a) V_{ds} vs. I_{ds} under a 685 nm laser at 3 different powers. V_g = 0 V. (b) Power dependence on the photocurrent of the device at V_{ds} = 5 V, V_g = 0 V. The dependence on power was found to equal 0.92 ± 0.04. Red points are recorded data and the black dashed line is the fit. (c) V_g vs. I_{ds} plot at V_{ds} = 5 V shown on logarithmic scale with the dark measurement in black and 400 nW, 685 nm laser measurement in red. (d) The photoresponsivity as a function of gate voltage.

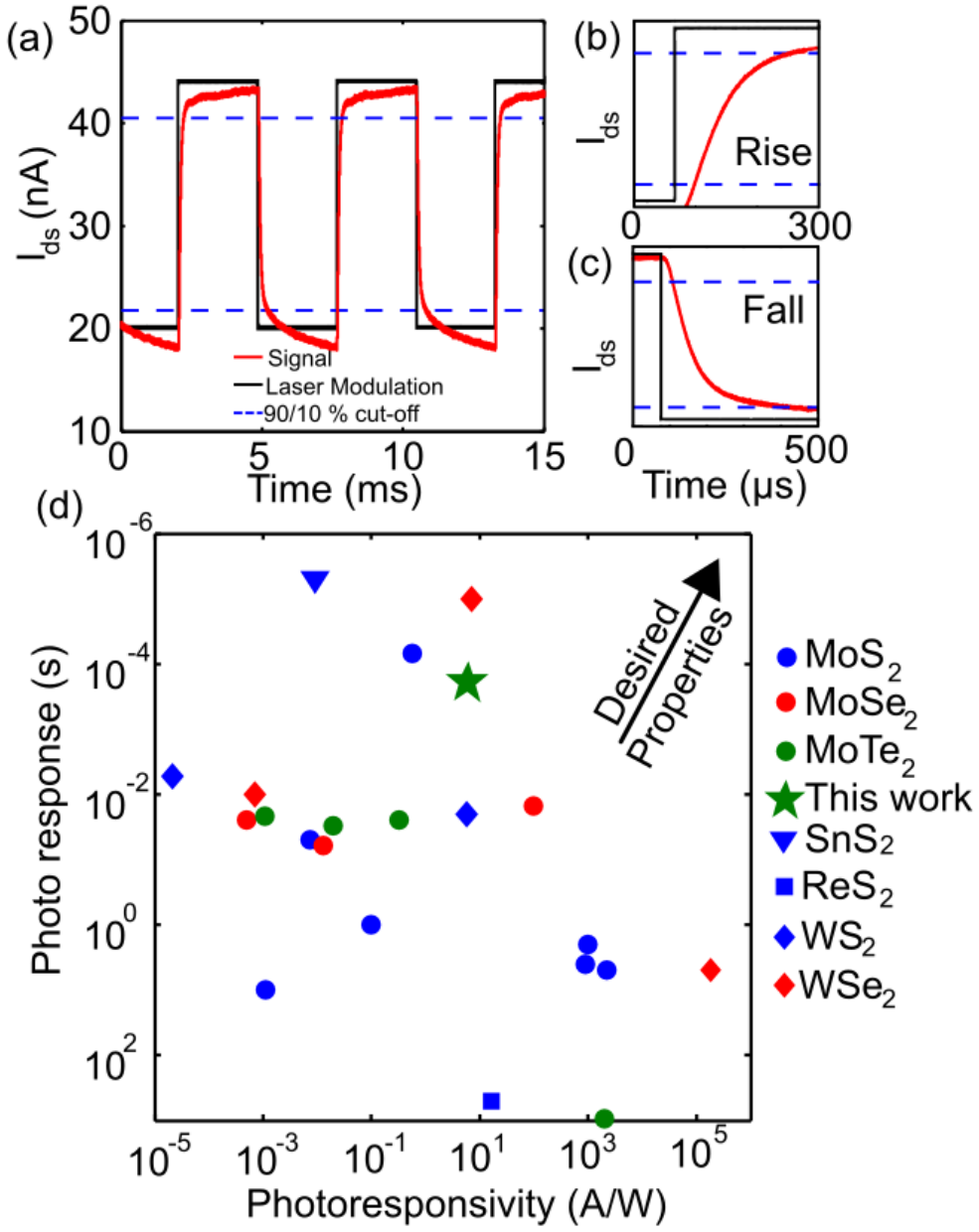

Figure 4. (a) Photoresponse of $MoTe_2$ device at V_{ds} = 5 V, V_g = 0 V modulated by a 178 Hz, 20 µW laser. (b) Zoomed in region of Figure 4a showing a rise time of 160 µs to get from 10% to 90% of the total signal. (c) Zoomed in region of Fig. 4(a) showing a fall time of 300 µs to get from 90% to 10% of the total signal. (d) Plot showing the photoresponsivity vs. photo response for TMDCs. References for work on TMDCs: MoS_2,[6,7,17,19,32,35,36] $MoSe_2$,[37–39] $MoTe_2$,[9,21–23] SnS_2,[33] ReS_2,[40] WS_2,[41,42] and WSe_2[26,43,44]. Our own work on $MoTe_2$ is highlighted by the green star.